Applied Numerical Mathematics 163 (2021) 167–181

Contents lists available at ScienceDirect

Applied Numerical Mathematics

www.elsevier.com/locate/apnum

Lax-Wendroff methods on highly non-uniform meshes. Dedicated to the Memory of Blair Swartz (1932–2019)

Richard Liska [a], Pavel Váchal [b,*], Burton Wendroff [b]

[a] Czech Technical University in Prague, Faculty of Nuclear Sciences and Physical Engineering, Břehová 7, 115 19 - Praha 1, Czech Republic
[b] Retired Fellow, Los Alamos National Laboratory, Los Alamos, NM, USA

ARTICLE INFO

Article history:
Received 25 August 2020
Received in revised form 22 January 2021
Accepted 23 January 2021
Available online 26 January 2021

Keywords:
Lax-Wendroff
Irregular grids
Truncation error
Supra-convergence

ABSTRACT

The standard Lax-Wendroff scheme with the conservative Lax-Friedrichs nodal predictor on highly non-uniform meshes produces serious oscillations, making it useless on such meshes. Wendroff and White (1989) [13] proposed two versions (WW and WWJp) with different predictors which work robustly on such meshes. Both WW and WWJp are second order accurate. We investigate how these methods behave on highly non-uniform meshes of three types (Pike, cluster and van der Corput) for 1D smooth solutions of the Burgers and the Euler equations. The WW and WWJp methods are extended to 2D and tested on smooth solutions of the Euler equations on 2D meshes created by the Cartesian product of 1D highly non-uniform meshes. We have not been able to find any significant difference between the WW and WWJp results, thus the simpler WW should be preferred.

1. Foreword by Burton Wendroff

This paper is about a version of the Lax-Wendroff (LW) method introduced in 1989 by A.B. White and me (BW) in [13] that, although often cited as a theoretical result, seems to have escaped notice as being a more robust scheme than LW. But first, a little history. In our 1960 and 1964 papers Lax and I derived a 2nd order stable scheme, the construction of which involved the Taylor expansion

$$u^{n+1} = u^n + \Delta t\, u_t^n + \frac{1}{2}\Delta t^2\, u_{tt}^n + \cdots$$

If the system of differential equations has the form

$$u_t = H(u)$$

for some operator H, we accounted for the u_{tt} term by using

$$u_{tt} = H_u H.$$

This leads to a clearly impractical scheme.

* Corresponding author.
E-mail address: pavel.vachal@fjfi.cvut.cz (P. Váchal).

https://doi.org/10.1016/j.apnum.2021.01.014
0168-9274/

Richtmyer observed that the central time expansion

$$u^{n+1} = u^n + \Delta t\, u_t^{n+\frac{1}{2}} + O(\Delta t^3)$$

makes more sense, for then the order of accuracy will depend on the accuracy of the predicted $H(u^{n+\frac{1}{2}})$. If the data u is located at cell centers, this requires obtaining u at the cell nodes. Richtmyer proposed using the Lax-Friedrichs (LF) scheme to do this. With this, 2nd order accuracy can be obtained on uniform grids for systems of hyperbolic conservation laws in one or two dimensions. LF uses averaging of the cell data at time t_n to get nodal data at that time. Although not in so many words, WW proposed using linear interpolation (in one dimension) to do this for any grids, and they applied this to Burgers' equation. Unfortunately, there are typos and gaps in that paper making exact reproducing of the results impossible, and equally unfortunate is the fact that I have neither records nor memory of the missing pieces. We have tried to remedy this situation in this paper.

1.1. Supra-convergence

Wendroff and White [13] actually presented a preliminary version of their work at a Hyperbolic Conference in 1988 [12], and there and in the 1989 paper the notion "supra-convergence" appears. Paraphrasing from [12], a difference scheme is supra-convergent if the global accuracy is of higher order than the local error would imply. The term supra-convergence appears for the first time in [3], although the phenomenon was observed earlier. My long-time friend, co-worker and one of the co-authors of [3], Blair Swartz, coined the term, which has since caught on in numerous publications. Blair passed away in 2019, and we have taken the opportunity to dedicate this work to his memory.

2. Introduction

What is commonly referred to as the Lax-Wendroff (LW) scheme for the numerical integration of systems of hyperbolic conservation laws is R.D. Richtmyer's [6] two-step version. To illustrate, consider

$$u_t + f(u)_x = 0, \qquad u(x,0) = g(x). \tag{1}$$

Cell-centered data $U^n_{i+\frac{1}{2}}$ is given at time t_n on cells

$$x_i < x_{i+1}, \qquad h_{i+\frac{1}{2}} = x_{i+1} - x_i.$$

The time-centered advance of the cell data, namely

$$U^{n+1}_{i+\frac{1}{2}} = U^n_{i+\frac{1}{2}} - \frac{\Delta t}{h_{i+\frac{1}{2}}}\left(f(U^{n+\frac{1}{2}}_{i+1}) - f(U^{n+\frac{1}{2}}_{i})\right), \tag{2}$$

needs nodal data $U^{n+\frac{1}{2}}_i$, which LW obtains using Lax-Friedrichs (LF), that is,

$$U^{n+\frac{1}{2}}_i = U^n_i - \frac{\Delta t}{2h_i}\left(f(U^n_{i+\frac{1}{2}}) - f(U^n_{i-\frac{1}{2}})\right), \tag{3}$$

where

$$U^n_i = \frac{h_{i+\frac{1}{2}}U^n_{i+\frac{1}{2}} + h_{i-\frac{1}{2}}U^n_{i-\frac{1}{2}}}{2h_i} \tag{4}$$

with

$$h_i = \frac{h_{i+\frac{1}{2}} + h_{i-\frac{1}{2}}}{2}.$$

Setting

$$\phi(U^n) = U^n_{i+\frac{1}{2}} - \frac{\Delta t}{h_{i+\frac{1}{2}}}\left(f(U^{n+\frac{1}{2}}_{i+1}) - f(U^{n+\frac{1}{2}}_{i})\right)$$

in the case of a uniform grid,

$$h_{i+\frac{1}{2}} = \Delta x \qquad \text{for all } i,$$

and smooth solution $u(x_{i+\frac{1}{2}}, t^n) \equiv u^n_{i+\frac{1}{2}}$ of (1) it is known [7], that the truncation error,

$$TE = u^n_{i+\frac{1}{2}} - \phi(u^n), \tag{5}$$

is second order:

$$TE = \Delta t\ O(\Delta x^2).$$

This means that where linear stability theory applies, for the conditionally stable LW, with for some constant A

$$\Delta t < A\Delta x,$$

at the final time $N\Delta t$, there is 2nd order convergence:

$$\left\| U^N - u^N \right\| = O(\Delta x^2),$$

typically for the L2 norm.

Second order convergence for nonlinear systems like the Euler equations is known to occur not only for uniform grids but also for smoothly varying grids and Lagrangian coordinate versions of LW [1]. This is not the case for arbitrary grids, where LW can even be inconsistent, see the truncation error of LW (14). We turn to this next.

2.1. The WW and WWJp schemes

In [13] A.B. White Jr. and one of the current authors (BW) introduced two schemes for conservation laws that we will call WWJp and WW. Both schemes use (2), but instead of (4) WWJp uses

$$U^n_i = \frac{h_{i-\frac{1}{2}} U^n_{i+\frac{1}{2}} + h_{i+\frac{1}{2}} U^n_{i-\frac{1}{2}}}{2h_i}, \tag{6}$$

and instead of (3) it uses

$$U^{n+\frac{1}{2}}_i = U^n_i - \frac{\Delta t}{2h_i} f_u(U^n_i) \left(U^n_{i+\frac{1}{2}} - U^n_{i-\frac{1}{2}} \right). \tag{7}$$

The WW scheme uses (6) and (3). (NOTE: (6) first appeared in [12], where what we call WW is called LW, but that is not standard practice.) Note that this interchange of weights is the result of using linear interpolation of the cell centered $U^n_{i+\frac{1}{2}}$ and $U^n_{i-\frac{1}{2}}$ to get U^n_i. It is also the result of inverse weight averaging

$$U^n_i = \frac{h^{-1}_{i+\frac{1}{2}} U^n_{i+\frac{1}{2}} + h^{-1}_{i-\frac{1}{2}} U^n_{i-\frac{1}{2}}}{h^{-1}_{i+\frac{1}{2}} + h^{-1}_{i-\frac{1}{2}}}. \tag{8}$$

This apparently slight difference between LW and WW (that is, (4) versus (6)) has profound implications. As a preliminary illustration of this point, we show in Fig. 1 an exact solution of Burgers' equation together with the solution obtained by LW and WW on a highly non-uniform grid. Clearly, LW is wrong while WW looks perfect at this scale.

3. Truncation error analysis

Next, consider the notion of truncation error. For a difference scheme of the form

$$U^{n+1}_{i+\frac{1}{2}} - \phi(U^n) = 0 \tag{9}$$

there is a *direct* truncation error obtained by substituting an exact smooth solution $u(x,t)$ of the differential equations into (9) to obtain

$$TEd \equiv u^{n+1}_{i+\frac{1}{2}} - \phi(u^n). \tag{10}$$

There is an *indirect* truncation error obtained by defining a "target function" $w(x,t)$ which is in this case, following [13],

$$w(x_{i+\frac{1}{2}}, t) = u(x_{i+\frac{1}{2}}, t) - \frac{1}{8} h^2_{i+\frac{1}{2}} (u_{xx})_{i+\frac{1}{2}} \tag{11}$$

and then

$$TEi \equiv w^{n+1}_{i+\frac{1}{2}} - \phi(w^n). \tag{12}$$

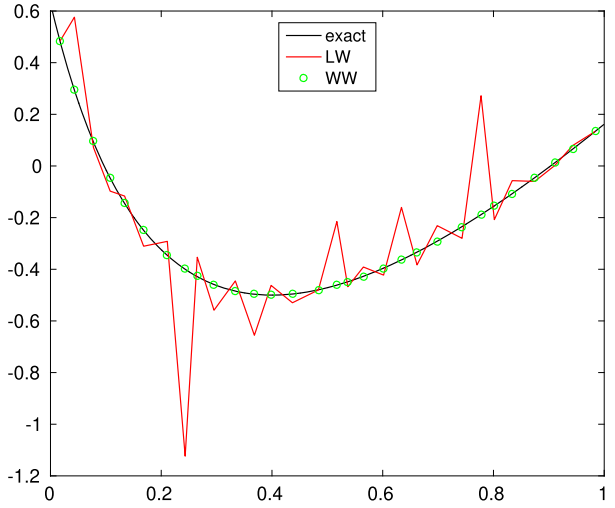

Fig. 1. Solution of Burgers' equation with initial condition $u(x,0) = -\frac{1}{4} + 2\left(x - \frac{1}{2}\right)^2 - \frac{1}{4}\sin(\pi x)$, i.e., (27) with $c = -1/4$, van der Corput grid, 30 cells, final time $T = 0.2$.

The target (11) originates at the Taylor expansion of the WW weighting (6)

$$\frac{h_{i-\frac{1}{2}}U_{i+\frac{1}{2}} + h_{i+\frac{1}{2}}U_{i-\frac{1}{2}}}{2h_i} = u_i + \frac{h_{i+\frac{1}{2}}}{2h_i}\frac{1}{8}h_{i-\frac{1}{2}}^2 u_{i,xx} + \frac{h_{i-\frac{1}{2}}}{2h_i}\frac{1}{8}h_{i+\frac{1}{2}}^2 u_{i,xx} + O(h^3). \tag{13}$$

Note, that the target (11) works for WWJp, however we have not succeeded to find a target working for WW.

The classic LW is known to be 1st order (or worse) for general non-uniform grids. Its direct truncation error is

$$\frac{1}{\Delta t}TEd(LW) = \frac{h_{i+\frac{3}{2}} - 2h_{i+\frac{1}{2}} + h_{i-\frac{1}{2}}}{2h_{i+\frac{1}{2}}} f_u u_x + O(\Delta t) + O(h), \tag{14}$$

where

$$h = \max h_{i+\frac{1}{2}},$$

so LW is not consistent and basically unacceptable on general non-uniform grids. We have used Maple[1] to compute the truncation errors.

In [13] it is shown that TEd(WW) and TEd(WWJp) are 1st order, but TEi(WWJp) is 2nd order, while TEi(WW) remains 1st order. In fact using Maple, these truncation errors are

$$\begin{aligned}
\frac{1}{\Delta t}TEd(WW) = &-\frac{\Delta t}{8h_{i+\frac{1}{2}}}\left(h_{i+\frac{3}{2}} - 2h_{i+\frac{1}{2}} + h_{i-\frac{1}{2}}\right) f_u\left(f_u u_{xx} + (f_{uu}u_x)u_x\right) \\
&+ \frac{1}{8}\left(h_{i+\frac{3}{2}} - h_{i-\frac{1}{2}}\right) f_u u_{xx} + O(\Delta t^2) + O(h^2), \\
\frac{1}{\Delta t}TEd(WWJp) = &-\frac{\Delta t}{8h_{i+\frac{1}{2}}}\left(h_{i+\frac{3}{2}} - 2h_{i+\frac{1}{2}} + h_{i-\frac{1}{2}}\right) f_u f_u u_{xx} \\
&+ \frac{1}{8}\left(h_{i+\frac{3}{2}} - h_{i-\frac{1}{2}}\right) f_u u_{xx} + O(\Delta t^2) + O(h^2),
\end{aligned}$$

but

$$\frac{1}{\Delta t}TEi(WWJp) = O(\Delta t^2) + O(h^2), \tag{15}$$

which together with (11) indicates 2nd order accuracy. This is not the case for WW, since

$$\frac{1}{\Delta t}TEi(WW) = -\frac{\Delta t}{8h_{i+\frac{1}{2}}}\left(h_{i+\frac{3}{2}} - 2h_{i+\frac{1}{2}} + h_{i-\frac{1}{2}}\right) f_u(f_{uu}u_x)u_x + O(\Delta t^2) + O(h^2). \tag{16}$$

[1] Maple is a trademark of Waterloo Maple Inc.

We have verified, that the presented truncation errors are correct also for systems, for which the Jacobi matrix f_u is a 2D tensor and f_{uu} is a 3D tensor.

3.1. Truncation error of the WW scheme

To show that WW is also 2nd order accurate, we need to proceed differently. For the conservation law

$$u_t + f(u)_x = 0, \tag{17}$$

set

$$p(x,t) = f(u(x,t)). \tag{18}$$

There is a differential equation for p,

$$p_t + f_u^2 u_x = 0. \tag{19}$$

Consider then the system for (u, p), (19) and

$$u_t + p_x = 0 \tag{20}$$

Assume that for given smooth initial data $u(x,0)$ and $p(x,0) = f(u(x,0))$ the system has a unique smooth solution pair $u(x,t)$ and $p(x,t) = f(u(x,t))$, up to some finite time. The initial conditions are

$$U^0_{i+\frac{1}{2}} = u(x_{i+\frac{1}{2}}, 0),$$
$$P^0_{i+\frac{1}{2}} = f(U^0_{i+\frac{1}{2}}).$$

Applying a suitably modified WWJp scheme to this system, for (20) the nodal u-component predictor is

$$U_i^{n+\frac{1}{2}} = U_i^n + \frac{\Delta t}{2h_i}\left(P^n_{i+\frac{1}{2}} - P^n_{i-\frac{1}{2}}\right), \tag{21}$$

where U_i^n is given by (6). Now we should use for the cell u-component corrector

$$U^{n+1}_{i+\frac{1}{2}} = U^n_{i+\frac{1}{2}} - \frac{\Delta t}{h_{i+\frac{1}{2}}}\left(P_{i+1}^{n+\frac{1}{2}} - P^{n+\frac{1}{2}}\right), \tag{22}$$

where $P_i^{n+\frac{1}{2}}$ is the nodal P predictor from (19). Instead we will use

$$U^{n+1}_{i+\frac{1}{2}} = U^n_{i+\frac{1}{2}} - \frac{\Delta t}{h_{i+\frac{1}{2}}}\left(f(U_{i+1}^{n+\frac{1}{2}}) - f(U_i^{n+\frac{1}{2}})\right) \tag{23}$$

and

$$P^{n+1}_{i+\frac{1}{2}} = f(U^{n+1}_{i+\frac{1}{2}}). \tag{24}$$

The key point here is that now we can use the two-component target

$$\left(u - \frac{1}{8}h^2 u_{xx}\,,\ p - \frac{1}{8}h^2 p_{xx}\right)_{i+\frac{1}{2}} \tag{25}$$

substituted for U, P into (21) and (23) to get the truncation error for u. Using Maple we find that this indirect truncation error is 2nd order. The scheme itself, i.e. predictor (21) with (6) and corrector (23) with (24), is WW for u and (17) and we have proved, that WW is 2nd order, which holds also for systems.

4. Pike, clusters and van der Corput grids

One reason we are unable to reproduce the numerical results of [13] is that the grids are called two-periodic without definition. However, it seems likely that they are like those used in the cited paper by J. Pike [5]. Since we do not know that for sure, in addition to the Pike grids we will also use a grid class based on the van der Corput (vdC) pseudo-random sequence, and a class consisting of clusters of uniform sub-grids representing the possibility of a material interface at a large jump in grid size.

There are two important differences between Pike, clusters and vdC. For Pike, the ratio of largest interval to smallest for a grid of k cells is independent of k, while for vdC this ratio is $O(k)$. The other difference is that the time step Δt for Pike is $O(1/k)$, for vdC Δt is $O(1/k^2)$.

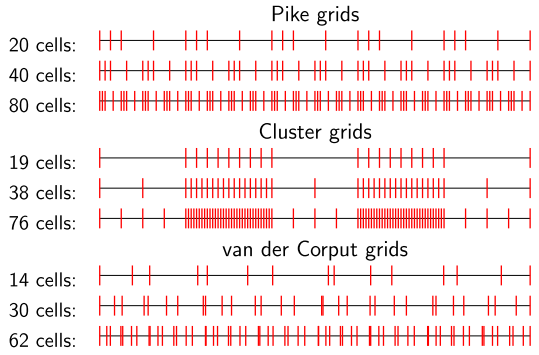

Fig. 2. Pike, cluster and van der Corput grids.

4.1. Pike grids

We define Pike as repeated groups of four intervals each,

$$\left[\frac{\Delta x}{2}, \frac{\Delta x}{2}, 3\frac{\Delta x}{2}, 3\frac{\Delta x}{2}, \cdots\right],$$

where Δx is the interval size for a uniform grid of four cells. The total length of the Pike group of four is

$$4\Delta x.$$

If there are m groups, say for the unit interval, then

$$\Delta x = 1/4m$$

and the number of cells is

$$k = 4m.$$

Pike grids consisting of 20, 40 and 80 cells can be seen in the upper part of Fig. 2. In 1D convergence tables below we use Pike grids with $m = 10; 20; 40; 80; 160; 320; 640$.

4.2. Cluster grids

These grids have regions of uniformity with a jump at the interface.

So, for example, each of the grids shown in the middle portion of Fig. 2 consists of five regular clusters, out of which two (namely the second and the fourth) are refined by a factor 8. That is, the cell lengths are

$$\Big[\underbrace{\Delta x, \cdots, \Delta x}_{m \text{ cells}}, \underbrace{\tfrac{\Delta x}{8}, \cdots, \tfrac{\Delta x}{8}}_{8m \text{ cells}}, \underbrace{\Delta x, \cdots, \Delta x}_{m \text{ cells}}, \underbrace{\tfrac{\Delta x}{8}, \cdots, \tfrac{\Delta x}{8}}_{8m \text{ cells}}, \underbrace{\Delta x, \cdots, \Delta x}_{m \text{ cells}}\Big],$$

where m is the number of cells in each sparse (not refined) cluster, the number of cells is

$$k = 19m$$

and on a unit interval

$$\Delta x = \frac{1}{5m}.$$

The examples in Fig. 2 show the grids with $m = 1$ (19 cells), $m = 2$ (38 cells) and $m = 4$ (76 cells). In 1D convergence tables below we use the cluster grids with $m = 2; 4; 8; 16; 32; 64; 128$.

The intention here is to mimic local grid refinement.

4.3. Van der Corput grids

The van der Corput (vdC) sequences (see e.g. [8] p. 250) of base 2 can be looked at as a suitably normalized rearrangement of the odd integers up to 2^m, $m = 4, 5, \cdots$. This rearrangement always puts the smallest integer - 1 - first and the largest - $2^m - 1$ - last. We eliminate this bias by not including the smallest and largest. Then for each m we would have a grid of k cells,

$$k = 2^{m-1} - 2.$$

The total of the odd integers from 1 to 2^m excluding 1 and $2^m - 1$ is

$$\sum_{l=1}^{2^{m-1}} (2l-1) - 1 - (2^m - 1) = 2^{m-1}k.$$

So, the grid will be a rearrangement of the set of intervals

$$\frac{\Delta x}{2^{m-1}}\left[3, 5, \cdots, 2^m - 3\right]$$

for each of which the total length is $k\Delta x$.

The actual arrangement of the cells can be obtained as follows. Let

$$n_i = 2^{m-1} + i, \qquad i = 1, \cdots, 2^{m-1} - 2.$$

If the base two expansion of n_i is

$$n_i = \sum_{l=0}^{m-1} a_l 2^l,$$

then the vdC integer sequence is

$$\nu_i = \sum_{l=0}^{m-1} a_l 2^{m-1-l}.$$

Then

$$h_{i-\frac{1}{2}} = \frac{\Delta x}{2^{m-1}} \nu_i, \qquad i = 1, 2, \cdots, 2^{m-1} - 2.$$

The bottom Section of Fig. 2 shows the van der Corput grids for $m = 5$ (14 cells), $m = 6$ (30 cells) and $m = 7$ (62 cells). As an example, the van der Corput grid for $m = 4$ (6 cells) on the unit interval $(0, 1)$ has cell volumes

$$\left(\frac{9}{8}, \frac{5}{8}, \frac{13}{8}, \frac{3}{8}, \frac{11}{8}, \frac{7}{8}\right)\frac{1}{6}.$$

In 1D convergence tables below we use the van der Corput grids with $m = 6; 7; 8; 9; 10; 11; 12$.

5. Numerical results

5.1. Burgers' equation

Another reason why we are unable to reproduce the numerical results of [13] is that the test problem as presented makes no sense. However, it seems likely that the intended conservation law is Burgers' equation

$$u_t + \frac{1}{2}(u^2)_x = 0 \tag{26}$$

with the initial condition

$$u(x, 0) = c + 2\left(x - \frac{1}{2}\right)^2 - \frac{1}{4}\sin \pi x, \tag{27}$$

where $c = 1/2$ or $c = -1/4$, as stated in [13]. Since we do not know just what grids were used in [13], in addition to the Pike grids we will also use the other two grid classes from Section 4, namely the cluster grids and the van der Corput grids.

Assuming that we are correct about Burgers (26) being the intended equation and (27) being the initial data in [13], we consider the incorrect claim made there that with $c = -1/4$ in (27) WW is only first order in the max norm. With this initial condition the exact solution at any (x, t) is obtained by the method of characteristics (e.g. [4]) on the interval $x \in (0, 1)$. The boundary condition is exact. The final time is $T = 0.2$. The timestep is calculated at every step n as

$$\Delta t^n = C_{\mathrm{CFL}} \min_i \frac{\Delta x_{i+\frac{1}{2}}}{\max\left(\left|U^n_{i+\frac{1}{2}}\right|, \varepsilon\right)},$$

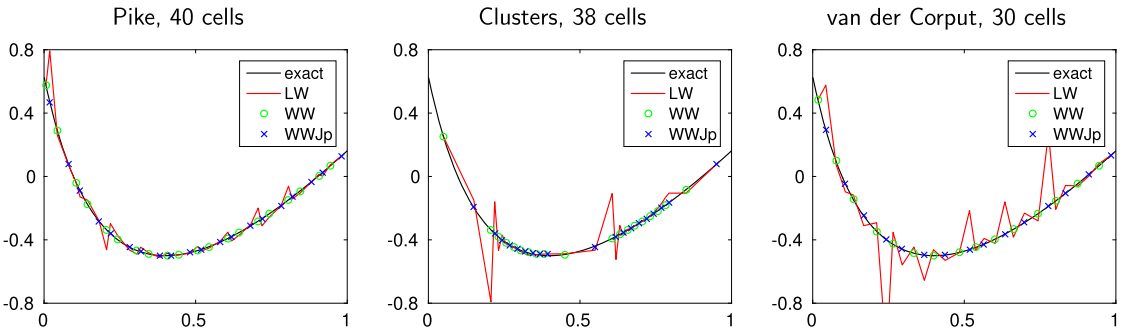

Fig. 3. Burgers' equation, test (27) with $c = -1/4$. As both the WW and WWJp values lie visually on the exact curve, only some of their cell-centered values are shown: in odd cells for WW, in even cells for WWJp.

Table 1
Numerical order of convergence in the $L_{\max}$ norm for Burgers' equation with the initial condition (27) with $c = -1/4$.

Level of ref.	No. of cells			Numerical order of convergence					
	Pike	cluster	vdC	Pike		cluster		vdC	
				WW	WWJp	WW	WWJp	WW	WWJp
1	40	38	30	N / A	N / A	N / A	N / A	N / A	N / A
2	80	76	62	0.86	1.01	0.03	0.03	1.81	2.10
3	160	152	126	2.05	1.90	1.68	1.68	1.01	1.03
4	320	304	254	1.81	1.85	1.80	1.80	1.84	1.83
5	640	608	510	1.81	1.92	1.93	1.93	1.78	1.77
6	1280	1216	1022	1.78	1.95	1.97	1.97	2.00	1.93
7	2560	2432	2046	1.89	1.98	1.99	1.99	2.10	2.03

with the CFL number set to $C_{\mathrm{CFL}} = 0.45$ and the technical threshold $\varepsilon = 10^{-14}$ used to avoid the division by zero for a possible zero $|U^n_{i+\frac{1}{2}}|$.

Fig. 3 presents a comparison of the exact solution with LW, WW and WWJp on Pike, clusters and vdC for relatively coarse grids. As in Fig. 1, LW is unacceptable, while both WW and WWJp are indistinguishable from the exact solution at this scale. Table 1 shows the $L_{\max}$ numerical order of convergence (NOC) for WW and WWJp. Both show second order accuracy and their results are very close.

5.2. Isentropic Euler

Going somewhat beyond [13], we compare here WW and WWJp applied to the isentropic Euler equations, for our three grid types. A test with exact solution is taken from [9,11,10] and will be referred to as Vilar's smooth test here. The equations are

$$\begin{aligned} \rho_t + (\rho v)_x &= 0, \\ (\rho v)_t + (\rho v^2)_x + p_x &= 0, \\ p = p(\rho) &= \rho^\gamma. \end{aligned}$$

Setting

$$u = (\rho, \rho v)$$

and

$$f(u) = (\rho v, (\rho v)^2/\rho + p(\rho)),$$

we have a system (1). The Jacobian f_u is

$$\begin{pmatrix} 0 & 1 \\ v^2 + p' & 2v \end{pmatrix}.$$

The initial condition is

$$\begin{aligned} \rho(x, 0) &= 1 + \frac{1}{10}\sin(2\pi x), \\ v(x, 0) &= 0 \end{aligned}$$

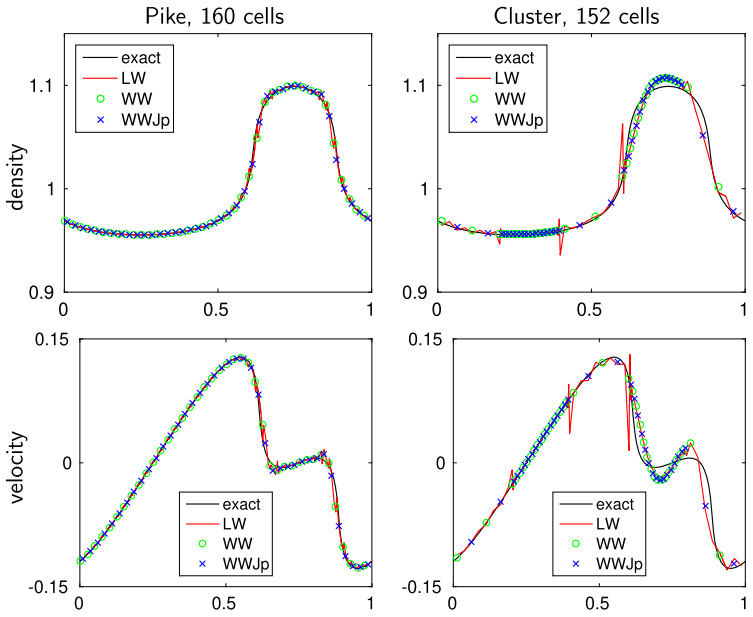

Fig. 4. Isentropic Euler, Vilar's smooth test. Top: density; bottom: velocity. Left: Pike's grid, 160 cells; Right: cluster grid, 152 cells. For better visibility, only values in cells 1,5,9,... are shown for WW and only values in cells 3,7,11,... for WWJp.

and a special choice $\gamma = 3$ reduces the problem to a set of two Burgers' equations, for which an exact solution can be found by the method of characteristics [11,10]. We run the calculation up to final time $T = 0.8$ on the domain $x \in (0, 1)$ with the periodic boundary conditions. The timestep is calculated at every step n as

$$\Delta t^n = C_{\mathrm{CFL}} \min_i \frac{\Delta x_{i+\frac{1}{2}}}{\max\left(\left|v_{i+\frac{1}{2}} - a_{i+\frac{1}{2}}\right|, \left|v_{i+\frac{1}{2}} + a_{i+\frac{1}{2}}\right|\right)}$$

with $a_{i+\frac{1}{2}}$ being the speed of sound,

$$a_{i+\frac{1}{2}} = \sqrt{\gamma\, \rho_{i+\frac{1}{2}}^{\gamma-1}},$$

and the CFL number is set again to $C_{\mathrm{CFL}} = 0.45$.

The results on Pike's grid with 160 cells and on the cluster grid with 152 cells are shown in Fig. 4. LW is unacceptable again. Table 2 shows the numerical order of convergence in the $L_{\max}$ norm for WW and WWJp. Both schemes show second order and their results are very close again.

6. Two dimensions

The system of equations is now

$$u_t + f_x + g_y = 0. \tag{28}$$

Consider a non-uniform rectangular grid formed by the intersections of a family of lines parallel to the y-axis separated by lengths $h_{i+\frac{1}{2}}$ with a family of lines parallel to the x-axis separated by lengths $k_{j+\frac{1}{2}}$. The cells $(i+\frac{1}{2}, j+\frac{1}{2})$ have width $\Delta x = h_{i+\frac{1}{2}}$, height $\Delta y = k_{j+\frac{1}{2}}$, and area $A_{i+\frac{1}{2},j+\frac{1}{2}} = h_{i+\frac{1}{2}} k_{j+\frac{1}{2}}$. For later use, let

$$h_i = \frac{1}{2}\left(h_{i+\frac{1}{2}} + h_{i-\frac{1}{2}}\right), \qquad k_j = \frac{1}{2}\left(k_{j+\frac{1}{2}} + k_{j-\frac{1}{2}}\right).$$

The cell data at time t_n, $U^n_{i+\frac{1}{2},j+\frac{1}{2}}$, are assumed to be located at the cell centers. As in Section 2, we will need data at the nodes, $U^n_{i,j}$. It is easy to see that if we define the nodal data as the bilinear interpolant of the surrounding four cells, then

$$A_{i,j} U^n_{i,j} = \frac{1}{4}\left(A_{i-\frac{1}{2},j+\frac{1}{2}} U^n_{i+\frac{1}{2},j-\frac{1}{2}} + A_{i+\frac{1}{2},j-\frac{1}{2}} U^n_{i-\frac{1}{2},j+\frac{1}{2}} + A_{i+\frac{1}{2},j+\frac{1}{2}} U^n_{i-\frac{1}{2},j-\frac{1}{2}} + A_{i-\frac{1}{2},j-\frac{1}{2}} U^n_{i+\frac{1}{2},j+\frac{1}{2}}\right) \tag{29}$$

Table 2
Numerical order of convergence in the $L_{\max}$ norm for isentropic Euler, Vilar's smooth test.

Level of ref.	No. of cells			Numerical convergence of density					
	Pike	cluster	vdC	Pike		cluster		vdC	
				WW	WWJp	WW	WWJp	WW	WWJp
1	40	38	30	N / A	N / A	N / A	N / A	N / A	N / A
2	80	76	62	0.56	0.54	0.71	0.71	0.52	0.52
3	160	152	126	0.83	0.83	0.40	0.40	0.75	0.75
4	320	304	254	1.04	1.04	0.84	0.84	1.08	1.08
5	640	608	510	1.37	1.38	0.87	0.86	1.34	1.34
6	1280	1216	1022	1.66	1.66	1.24	1.24	1.67	1.67
7	2560	2432	2046	1.90	1.90	1.56	1.56	1.88	1.88

Level of ref.	No. of cells			Numerical convergence of velocity					
	Pike	cluster	vdC	Pike		cluster		vdC	
				WW	WWJp	WW	WWJp	WW	WWJp
1	40	38	30	N / A	N / A	N / A	N / A	N / A	N / A
2	80	76	62	0.66	0.64	0.43	0.44	0.73	0.73
3	160	152	126	0.87	0.87	0.87	0.87	0.84	0.84
4	320	304	254	1.05	1.05	0.96	0.96	1.08	1.08
5	640	608	510	1.37	1.38	0.86	0.86	1.34	1.34
6	1280	1216	1022	1.66	1.66	1.24	1.24	1.67	1.67
7	2560	2432	2046	1.90	1.90	1.56	1.56	1.87	1.87

with

$$A_{i,j} = \frac{1}{4}\left(A_{i-\frac{1}{2},j+\frac{1}{2}} + A_{i+\frac{1}{2},j-\frac{1}{2}} + A_{i+\frac{1}{2},j+\frac{1}{2}} + A_{i-\frac{1}{2},j-\frac{1}{2}}\right).$$

The nodal predictor will have the form

$$U^{n+\frac{1}{2}}_{i,j} = U^{n}_{i,j} - \frac{1}{2}\Delta t\left((f_x)_{i,j} + (g_y)_{i,j}\right)$$

with $(f_x)_{i,j}$ and $(g_y)_{i,j}$ defined by

$$(f_x)_{i,j} = \frac{f\left(U^n_{i+\frac{1}{2},j}\right) - f\left(U^n_{i-\frac{1}{2},j}\right)}{h_i},$$

$$(g_y)_{i,j} = \frac{g\left(U^n_{i,j+\frac{1}{2}}\right) - g\left(U^n_{i,j-\frac{1}{2}}\right)}{k_j},$$

where the values at the edges' centers are given by the linear interpolation from neighboring cells

$$U^n_{i+\frac{1}{2},j} = \frac{k_{j+\frac{1}{2}}U^n_{i+\frac{1}{2},j-\frac{1}{2}} + k_{j-\frac{1}{2}}U^n_{i+\frac{1}{2},j+\frac{1}{2}}}{2k_j},$$

$$U^n_{i,j+\frac{1}{2}} = \frac{h_{i+\frac{1}{2}}U^n_{i-\frac{1}{2},j+\frac{1}{2}} + h_{i-\frac{1}{2}}U^n_{i+\frac{1}{2},j+\frac{1}{2}}}{2h_i}.$$

With these definitions we can now write the WW 2D nodal predictor as

$$U^{n+\frac{1}{2}}_{i,j} = U^{n}_{i,j} - \frac{1}{2}\Delta t\,\frac{f\left(U^n_{i+\frac{1}{2},j}\right) - f\left(U^n_{i-\frac{1}{2},j}\right)}{h_i} - \frac{1}{2}\Delta t\,\frac{g\left(U^n_{i,j+\frac{1}{2}}\right) - g\left(U^n_{i,j-\frac{1}{2}}\right)}{k_j}.$$

The WWJp 2D nodal predictor will be

$$U^{n+\frac{1}{2}}_{i,j} = U^{n}_{i,j} - \frac{1}{2}\Delta t\, f_u(U^n_{i,j})\,\frac{U^n_{i+\frac{1}{2},j} - U^n_{i-\frac{1}{2},j}}{h_i} - \frac{1}{2}\Delta t\, g_u(U^n_{i,j})\,\frac{U^n_{i,j+\frac{1}{2}} - U^n_{i,j-\frac{1}{2}}}{k_j}.$$

The final corrector step is standard,

$$U^{n+1}_{i+\frac{1}{2},j+\frac{1}{2}} = U^{n}_{i+\frac{1}{2},j+\frac{1}{2}} - \frac{1}{2}\frac{\Delta t}{h_{i+\frac{1}{2}}}\left[f\left(U^{n+\frac{1}{2}}_{i+1,j}\right)+f\left(U^{n+\frac{1}{2}}_{i+1,j+1}\right)-f\left(U^{n+\frac{1}{2}}_{i,j}\right)-f\left(U^{n+\frac{1}{2}}_{i,j+1}\right)\right] - \frac{1}{2}\frac{\Delta t}{k_{j-\frac{1}{2}}}\left[g\left(U^{n+\frac{1}{2}}_{i,j+1}\right)+g\left(U^{n+\frac{1}{2}}_{i+1,j+1}\right)-g\left(U^{n+\frac{1}{2}}_{i,j}\right)-g\left(U^{n+\frac{1}{2}}_{i+1,j}\right)\right].$$

6.1. Reciprocal subcell area weighting for the nodal data

If we divide both sides of (29) by

$$h_{i-\frac{1}{2}}k_{j+\frac{1}{2}}h_{i+\frac{1}{2}}k_{j-\frac{1}{2}},$$

we will get

$$B_{i,j}U^{n}_{i,j} = \frac{1}{4}\left[\left(h_{i+\frac{1}{2}}k_{j-\frac{1}{2}}\right)^{-1}U^{n}_{i+\frac{1}{2},j-\frac{1}{2}}+\left(h_{i-\frac{1}{2}}k_{j+\frac{1}{2}}\right)^{-1}U^{n}_{i-\frac{1}{2},j+\frac{1}{2}} + \left(h_{i-\frac{1}{2}}k_{j-\frac{1}{2}}\right)^{-1}U^{n}_{i-\frac{1}{2},j-\frac{1}{2}}+\left(h_{i+\frac{1}{2}}k_{j+\frac{1}{2}}\right)^{-1}U^{n}_{i+\frac{1}{2},j+\frac{1}{2}}\right],$$

where

$$B_{i,j} = \frac{1}{4}\left[\left(h_{i-\frac{1}{2}}k_{j+\frac{1}{2}}\right)^{-1}+\left(h_{i+\frac{1}{2}}k_{j-\frac{1}{2}}\right)^{-1}+\left(h_{i+\frac{1}{2}}k_{j+\frac{1}{2}}\right)^{-1}+\left(h_{i-\frac{1}{2}}k_{j-\frac{1}{2}}\right)^{-1}\right].$$

Using p-c (point-cell) notation, the general situation would be, but now for any grid,

$$U^{n}_{p} = \frac{\sum_{c(p)}(A_{cp})^{-1}U_{cp}}{\sum_{c(p)}(A_{cp})^{-1}},$$

where A_{cp} are the subcell areas.

This inverse weighting has been used in a Lagrangian version of Lax-Wendroff in [2], where it has been shown to be effective on some classical test problems, such as Sod, Noh and Sedov, in both one and two dimensions.

6.2. Truncation error analysis

The direct and indirect truncation errors (TE) in 2D are defined in the same way as in 1D, (10) for direct TEd and (12) for indirect TEi. With

$$k = \max k_{j+\frac{1}{2}}$$

the direct TE for WW and WWJp on a rectangular grid are again computed by Maple to be

$$\begin{aligned}\frac{1}{\Delta t}TEd(WW)_{i+\frac{1}{2},j+\frac{1}{2}} =& -\frac{\Delta t}{8h_{i+\frac{1}{2}}}\left(h_{i+\frac{3}{2}}-2h_{i+\frac{1}{2}}+h_{i-\frac{1}{2}}\right)f_u\left(f_u u_{xx}+(f_{uu}u_x)u_x\right)\\ &+\frac{1}{8}\left(h_{i+\frac{3}{2}}-h_{i-\frac{1}{2}}\right)f_u u_{xx}\\ &-\frac{\Delta t}{8k_{j+\frac{1}{2}}}\left(k_{j+\frac{3}{2}}-2k_{j+\frac{1}{2}}+k_{j-\frac{1}{2}}\right)g_u\left(g_u u_{yy}+(g_{uu}u_y)u_y\right)\\ &+\frac{1}{8}\left(k_{j+\frac{3}{2}}-k_{j-\frac{1}{2}}\right)g_u u_{yy}+O(\Delta t^2)+O(h^2)+O(k^2),\\ \frac{1}{\Delta t}TEd(WWJp)_{i+\frac{1}{2},j+\frac{1}{2}} =& -\frac{\Delta t}{8h_{i+\frac{1}{2}}}\left(h_{i+\frac{3}{2}}-2h_{i+\frac{1}{2}}+h_{i-\frac{1}{2}}\right)f_u f_u u_{xx}\\ &+\frac{1}{8}\left(h_{i+\frac{3}{2}}-h_{i-\frac{1}{2}}\right)f_u u_{xx}\\ &-\frac{\Delta t}{8k_{j+\frac{1}{2}}}\left(k_{j+\frac{3}{2}}-2k_{j+\frac{1}{2}}+k_{j-\frac{1}{2}}\right)g_u g_u u_{yy}\\ &+\frac{1}{8}\left(k_{j+\frac{3}{2}}-k_{j-\frac{1}{2}}\right)g_u u_{yy}+O(\Delta t^2)+O(h^2)+O(k^2).\end{aligned}$$

Error analysis of the WW interpolant of the nodal value suggests the target

$$w(x_{i+\frac{1}{2}}, y_{j+\frac{1}{2}}, t) = u(x_{i+\frac{1}{2}}, y_{j+\frac{1}{2}}, t) - \frac{1}{8}\left(h^2_{i+\frac{1}{2}}(u_{xx})_{i+\frac{1}{2},j+\frac{1}{2}} + k^2_{j+\frac{1}{2}}(u_{yy})_{i+\frac{1}{2},j+\frac{1}{2}}\right).$$

With this target the indirect truncation error (12) for WWJp is however

$$\frac{1}{\Delta t} TEi(WWJp)_{i+\frac{1}{2},j+\frac{1}{2}} = O(\Delta t^2) + O(h^2) + O(k^2)$$

and thus WWJp is second order even in 2D. For WW the indirect truncation error is

$$\begin{aligned}\frac{1}{\Delta t} TEd(WW)_{i+\frac{1}{2},j+\frac{1}{2}} = &- \frac{\Delta t}{8h_{i+\frac{1}{2}}}\left(h_{i+\frac{3}{2}} - 2h_{i+\frac{1}{2}} + h_{i-\frac{1}{2}}\right) f_u(f_{uu}u_x)u_x \\ &- \frac{\Delta t}{8k_{j+\frac{1}{2}}}\left(k_{j+\frac{3}{2}} - 2k_{j+\frac{1}{2}} + k_{j-\frac{1}{2}}\right) g_u(g_{uu}u_y)u_y \\ &+ O(\Delta t^2) + O(h^2) + O(k^2),\end{aligned}$$

which is similar to the 1D case (16) and to show that WW is 2nd order also in 2D we need to proceed similarly like in 1D below (16).

6.2.1. Truncation error of the WW scheme in 2D

This is a straightforward extension of the procedure in Section 3.1 to 2D. Here we will have a system of three differential equations for the variables

$$u(x, y, t), \qquad p(x, y, t) = f(u(x, y, t)), \qquad q(x, y, t) = g(u(x, y, t)).$$

To this we apply a modified WWJp scheme with three-component target

$$\left(u - \frac{h^2}{8}u_{xx} - \frac{k^2}{8}u_{yy}\ ,\ p - \frac{h^2}{8}p_{xx} - \frac{k^2}{8}p_{yy}\ ,\ q - \frac{h^2}{8}q_{xx} - \frac{k^2}{8}q_{yy}\right)_{i+\frac{1}{2},j+\frac{1}{2}}$$

getting 2nd order accuracy again. We have verified the correctness of the truncation errors also for systems.

6.3. Euler equations

We consider here the standard compressible Euler equations including conservation laws for mass, momentum and energy.

We are going to solve the Euler equations on 2D orthogonal non-uniform meshes, which are created by the Cartesian product of 1D non-uniform meshes described in Section 4, i.e., Pike, cluster and van der Corput grids. For Pike grids we will use grids with 40 × 40, 80 × 80, 160 × 160, 320 × 320, 640 × 640, 1280 × 1280 and 2560 × 2560 cells. For cluster grids we will use grids with 38 × 38, 76 × 76, 152 × 152, 304 × 304, 608 × 608, 1216 × 1216 and 2432 × 2432 cells. For van der Corput grids we will use grids with 30 × 30, 62 × 62, 126 × 126, 254 × 254, 510 × 510 and 1022 × 1022 cells. We do not use van der Corput grid with 2046 × 2046 cells as such a grid implies a very small time step and thus needs too much time to compute.

6.3.1. Advection test

The initial conditions are

$$\rho_0(x, y) = 1 + \frac{1}{1000}\, e^{-400(x-x_0)^2}\, e^{-400(y-y_0)^2}, \qquad x_0 = y_0 = 0.5, \tag{30}$$

and

$$p_0(x, y) \equiv 1, \qquad v_0(x, y) = w_0(x, y) \equiv 1.$$

The solution of this problem is the density pulse advected by the constant velocity, i.e.,

$$\begin{aligned}&\rho(x, y, t) = 1 + \frac{1}{1000}\, e^{-400(x-x_0-v_0t)^2}\, e^{-400(y-y_0-w_0t)^2}, \\ &p(x, y, t) = p_0, \qquad v(x, y, t) = v_0, \qquad w(x, y, t) = w_0.\end{aligned}$$

The final time is now $T = 1.0$, we use $\gamma = 1.4$, $C_{\mathrm{CFL}} = 0.49$ and the periodic boundary conditions.

We have solved this advection problem as a special initial value problem for the full Euler equations. One can show that WW and WWJp keep the initially constant pressure and velocity for this problem at all time steps. Even further, it

Table 3
Numerical order of convergence in $L_{\max}$ norm for density for 2D Euler, advection test by WW and WWJp (their results are the same, so we present them only once).

Pike		cluster		vdC	
No. of cells	NOC	No. of cells	NOC	No. of cells	NOC
40 × 40	N / A	38 × 38	N / A	30 × 30	N / A
80 × 80	0.32	76 × 76	-2.16	62 × 62	-0.02
160 × 160	0.55	152 × 152	-0.36	126 × 126	0.60
320 × 320	1.20	304 × 304	0.35	254 × 254	1.13
640 × 640	1.94	608 × 608	0.99	510 × 510	1.92
1280 × 1280	2.03	1216 × 1216	1.85	1022 × 1022	1.94
2560 × 2560	2.01	2432 × 2432	2.03		

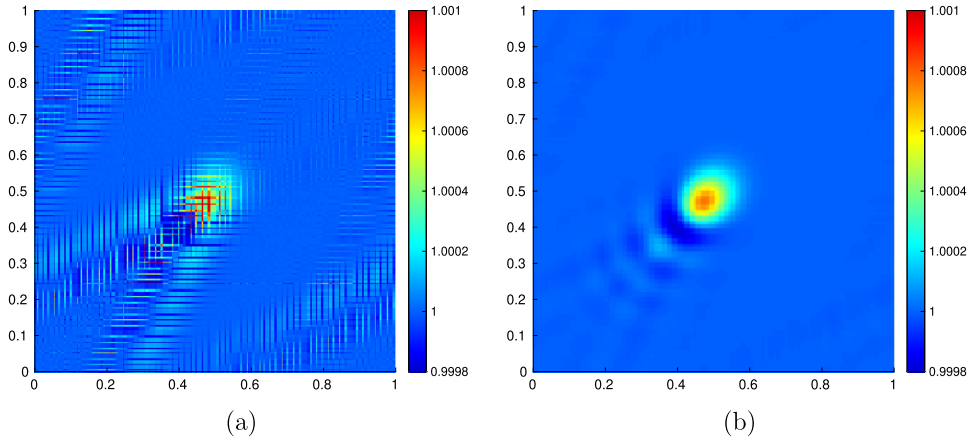

Fig. 5. Density for 2D Euler, advection test, van der Corput 126 × 126 mesh, by LW (a) and WW (b).

is not difficult to see that for this problem WW and WWJp are the same and mathematically fully equivalent to doing the advection problem for density. Therefore we only show the convergence rate for one of them. The numerical orders of convergence in the $L_{\max}$ norm for density for this test are presented in Table 3. The Table shows second order convergence. Owing to the small spatial size of the initial density bump, which cannot be resolved well on the coarse meshes, second order convergence is achieved only for finer meshes (from 640×640 resolution for Pike, from 1216×1216 resolution for cluster grid and from 510×510 resolution for vdC).

In Fig. 5 we present the density colormap for this test on the van der Corput 126 × 126 mesh by LW and WW. LW in Fig. 5(a) shows quite wild oscillations, similar to those in the 1D results in Fig. 3 for Burgers and in Fig. 4 for Euler. In the WW results in Fig. 5(b) the wild oscillations are missing, while the dispersive oscillations remain (the diameter of the bump (30) is about 0.15, while the greatest spatial step of this mesh is about 0.016, so the mesh is rather coarse for this bump).

6.3.2. Smooth test

This smooth 2D test has been inspired by the Vilar 1D test with exact solution [11,9], presented in Section 5.2. The Euler equations for a gamma-law gas with $\gamma = 3$ are solved on a unit square with the initial condition

$$\rho_0(x, y) = 1 + \tfrac{1}{10} \sin(2\pi x) \sin(2\pi y),$$
$$p_0(x, y) = \rho_0^\gamma = \rho_0^3, \qquad v_0(x, y) = w_0(x, y) = 0$$

and with periodic boundary conditions. The final time is $T = 0.8$ and CFL number is $C_{CFL} = 0.49$.

There is no exact solution for this problem. We have computed the reference solution on the high resolution uniform mesh with 10240 × 10240 cells by the WW scheme. For numerical order of convergence we use the deviation of the numerical solution on a given mesh from the high resolution solution on this mesh computed by bilinear interpolation of the reference solution from the uniform high resolution mesh to the given mesh. The numerical orders of convergence in the $L_{\max}$ norm for density for this test are presented in Table 4. The Table shows second order of convergence, which is again achieved for finer meshes.

In Fig. 6 we present the density colormap and its 1D horizontal cut along $y = 0.25$ with the reference solution for this test at the final time on the cluster 76 × 76 mesh by LW and WW. The LW results show again large oscillations in the smooth solution.

Table 4
Numerical order of convergence in $L_{\max}$ norm for density for 2D Euler, smooth test at the final time $T = 0.8$ by WW (the WWJp results are very close, so that their NOCs do not differ in the three decimal digits shown here).

Pike		cluster		vdC	
No. of cells	NOC	No. of cells	NOC	No. of cells	NOC
40 × 40	N / A	38 × 38	N / A	30 × 30	N / A
80 × 80	0.79	76 × 76	1.67	62 × 62	0.56
160 × 160	1.37	152 × 152	0.12	126 × 126	1.34
320 × 320	1.71	304 × 304	1.32	254 × 254	1.73
640 × 640	1.89	608 × 608	1.56	510 × 510	1.91
1280 × 1280	1.96	1216 × 1216	1.86	1022 × 1022	1.98
2560 × 2560	1.99	2432 × 2432	1.98		

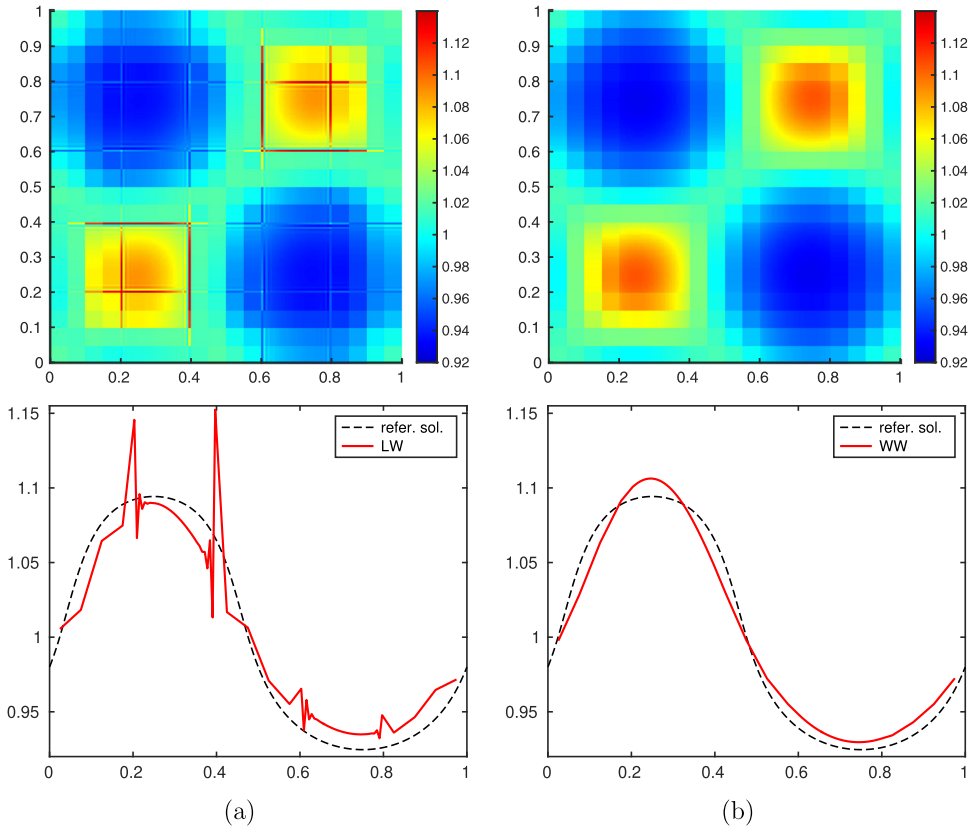

Fig. 6. Density for 2D Euler, smooth test, cluster 76 × 76 mesh, by LW (a) and WW (b). 2D colormap top and 1D horizontal cut at $y = 0.25$ with the reference solution bottom.

7. Conclusion

We have found that LW is not suitable for highly non-uniform grids and that WW and WWJp are robust and 2nd order accurate. We have extended WW and WWJp to 2D with the same properties. Numerical results of WW and WWJp are very close, which indicates that the simpler WW is to be preferred. At shock waves on non-uniform grids, WW and WWJp produce dispersive oscillations (similar to the classical LW oscillations on uniform grids), which should be treated by adding dissipation in some form, while LW crashes.

Acknowledgements

The authors would like to thank F. Vilar for fruitful discussions and valuable advice. R.L. and P.V. have been supported by the Czech Science Foundation project 18-20962S, by the project CZ.02.1.01/0.0/0.0/16_019/0000778 from European Regional Development Fund and by the Czech Ministry of Education project RVO 68407700.

References

[1] D. Fridrich, R. Liska, B. Wendroff, Some cell-centered Lagrangian Lax-Wendroff HLL hybrid schemes, J. Comput. Phys. 326 (2016) 878–892, https://doi.org/10.1016/j.jcp.2016.09.022.

[2] D. Fridrich, R. Liska, B. Wendroff, Cell-centered Lagrangian Lax-Wendroff HLL hybrid scheme in cylindrical geometry, J. Comput. Phys. 417 (2020) 109605, https://doi.org/10.1016/j.jcp.2020.10960.

[3] H.O. Kreiss, T.A. Manteuffel, B. Swartz, B. Wendroff, A.B. White Jr., Supra-convergent schemes on irregular grids, Math. Comput. 47 (1986) 537–554, https://doi.org/10.2307/2008171.

[4] R.J. LeVeque, Numerical Methods for Conservation Laws, Birkhäuser Verlag, Basel, 1992.

[5] J. Pike, Grid adaptive algorithms for the solution of the Euler equations on irregular grids, J. Comput. Phys. 71 (1987) 194–223, https://doi.org/10.1016/0021-9991(87)90027-1.

[6] R.D. Richtmyer, A Survey of Difference Methods for Non-Steady Fluid Dynamics, NCAR Tech. Notes 63-2 National Center for Atmospheric Research, Boulder, Colorado, 1963, https://doi.org/10.5065/D67P8WCQ.

[7] R.D. Richtmyer, K.W. Morton, Difference Methods for Initial Value Problems, 2nd edition, John Wiley and Sons, New York, 1967.

[8] E.F. Toro, Riemann Solvers and Numerical Methods for Fluid Dynamics. A Practical Introduction, 3rd edition, Springer-Verlag, Berlin, Heidelberg, 2009, https://doi.org/10.1007/978-3-540-49834-6.

[9] F. Vilar, A high-order Discontinuous Galerkin discretization for solving two-dimensional Lagrangian hydrodynamics, Ph.D. thesis, University Bordeaux I, 2012.

[10] F. Vilar, 2018, Personal communication.

[11] F. Vilar, P.-H. Maire, R. Abgrall, Cell-centered discontinuous Galerkin discretizations for two-dimensional scalar conservation laws on unstructured grids and for one-dimensional Lagrangian hydrodynamics, Comput. Fluids 46 (2011) 498–504, https://doi.org/10.1016/j.compfluid.2010.07.018.

[12] B. Wendroff, A.B. White Jr., Some supraconvergent schemes for hyperbolic equations on irregular grids, in: J. Ballmann, R. Jeltsch (Eds.), Nonlinear Hyperbolic Equations — Theory, Computation Methods, and Applications, in: Notes on Numerical Fluid Mechanics, vol. 24, Vieweg+Teubner Verlag, 1989, pp. 671–677, https://doi.org/10.1007/978-3-322-87869-4_65.

[13] B. Wendroff, A.B. White Jr., A supraconvergent scheme for nonlinear hyperbolic systems, Comput. Math. Appl. 18 (1989) 761–767, https://doi.org/10.1016/0898-1221(89)90232-0.